Single Carbon Nanotube Membranes: A Well-Defined Model for Studying Mass Transport through Nanoporous Materials

Li Sun*,† and Richard M. Crooks*,‡

Contribution from the Department of Chemistry, P.O. Box 30012, Texas A&M University, College Station, Texas 77842-3012

Received July 5, 2000. Revised Manuscript Received September 5, 2000

Abstract: This work represents the first study of mass transport phenomena within a nanotube and thus holds promise as a means of probing the properties of nanotube interiors. Multiwall carbon nanotubes are used as templates to fabricate single-pore membranes. These membranes are better experimental models for testing specific predictions of mass transport theories than arrays of nanopores because they require fewer adjustable parameters and they have well-defined geometry and chemical structures. Using polystyrene particles as probes, we demonstrate that quantitative information about fundamental modes of transport, such as hydrodynamic and electrophoretic flow, can be obtained using these single-pore membranes. Furthermore, time-resolved mass transport measurements can be achieved when the method of Coulter counting is used.

Introduction

In this report, we present the first quantitative study of mass transport through carbon nanotubes. Membranes containing only a single pore of about 150 nm diameter are fabricated, using multiwall carbon nanotubes as templates. Using the method of Coulter particle counting, we measured the transport rates of polystyrene probe particles (100 and 60 nm average diameters) through the single-pore membranes and analyzed our data with basic transport equations for flows across a cylindrical pore. This work has also pushed the particle size limit of a totally synthetic Coulter counter to a new record (about 50 nm). Further reduction in this limit is expected, which will bring us closer to the significant goal of constructing a totally synthetic molecular Coulter counter.

Mass transport in nanoporous media is of interest for many technologically important reasons, including: zeolite-based catalysis, separations employing membranes and chromatography, chemical analysis using porous coatings or microfluidic systems, and delivery of therapeutic molecules such as drugs and genes through cellular matrixes.[1−5] Transport in nanoporous media also poses interesting theoretical questions, because it differs from ordinary transport in bulk media. The differences arise largely because the interactions between a pore surface and the molecule being transported become increasingly important as the dimensions of the pore approach the size of the molecule. We believe that this unique size domain offers many opportunities where researchers in the field of surface chemistry, in particular the field of self-assembled monolayer chemistry, can make increasingly significant contributions to mass transport theories that incorporate specific pore surface chemistry in their descriptions. Toward this goal, we are exploring various means for fabricating and analyzing structurally well-defined nanopore models.[6]

Conventional nanopore models, such as dialysis membranes or polymeric woven-fiber membranes, contain a large array of pores with polydisperse structural parameters; that is, nanopores in these membranes exhibit a wide distribution in either shape, size, or surface chemistry. Quantitative data analysis for such models is difficult to implement because a complete description of a polydisperse structure is almost impossible without invoking many approximations and assumptions. More recently, materials containing arrays of pores with one or more monodisperse structural parameters have been reported: for example, membranes derived from etched polycarbonate (Nucleopore) or porous alumina membranes[7−9] and porous structures fabricated from monodisperse nanoscopic and mesoscopic objects.[10,11] These materials are potentially useful for mass transport studies because their relatively uniform pore geometry or surface chemistry would permit a more direct and quantitative structure/transport-rate correlation than materials having polydisperse pores. Indeed, encouraging results have already been reported, for example, by Martin and co-workers who demonstrated that array pores having molecular dimensions exhibit unique permselectivity and chemical selectivity.[7,8]

Membrane models containing monodisperse pore-arrays do have some drawbacks. First, it is difficult to ensure structural

* To whom correspondence should be directed.
† Telephone: 979-845-1595. Fax: 979-845-1399. E-mail: lisun@mail.chem.tamu.edu.
‡ Telephone: 979-845-5629. Fax: 979-845-1399. E-mail: crooks@tamu.edu.

(1) Chen, N. Y.; Thomas, F. D., Jr.; Smith, C. M. *Molecular Transport and Reaction in Zeolites*: *Design and Application of Shape Selective Catalysts*; VCH: New York, 1994.
(2) Crooks, R. M.; Ricco, A. J. *Acc. Chem. Res.* **1998**, *31*, 219−227.
(3) Schasfoort, R. B. M.; Schlautmann, S.; Hendrikse, J.; Van Den Berg, A. *Science* **1999**, *286*, 942−945.
(4) Bath, B. D.; Lee, R. D.; White, H. S. *Anal. Chem.* **1998**, *70*, 1047−1058.
(5) Ghadiri, M. R.; Granja, J. R.; Buehler, L. K. *Nature* **1994**, *369*, 301−304.
(6) Sun, L.; Crooks, R. M. *Langmuir* **1999**, *15*, 738−741.
(7) Nishizawa, M.; Menon, V. P.; Martin, C. R. *Science* **1995**, *268*, 700−702.
(8) Hulteen, J. C.; Jirage, K. B.; Martin, C. R. *J. Am. Chem. Soc.* **1998**, *120*, 6603−6604.
(9) Masuda, H.; Fukuda, K. *Science* **1995**, *268*, 1466−1468.
(10) Widawski, G.; Rawiso, M.; Francois, B. *Nature* **1994**, *369*, 387−389.
(11) Holland, B. T.; Blanford, C. F.; Stein, A. *Science* **1998**, *281*, 538−540.

10.1021/ja002429w CCC: $19.00
Published on Web 11/18/2000

uniformity in arrays containing 10^9 or more pores (assuming a pore diameter of 100 nm and a sample area of 1 cm^2), the problem is exacerbated as the pore dimensions become very small. For example, a track-etched polycarbonate membrane has three structural imperfections: (a) the pore length is not uniform because of variation in track tilt angle; (b) the pores are tapered and the pore surface is rough compared to the magnitude of the pore diameter; and (c) although uniform over a small patch of membrane surface, large-area membranes contain many defects such as those consisting of two tracks merged together due to their close proximity.[12] Second, under steady-state conditions, only a time-averaged transport rate can be determined because individual single-pore transport events cannot be temporally resolved from each other. Thus, statistical distribution in transport rate cannot be retrieved using an array-pore membrane model.

Single-pore membranes represent a new type of structural model for studying mass-transport kinetics. Since the number of variables required for complete structural description is less than for array-pore membranes, single-pore membranes are more useful for directly testing specific predictions of theory. The need for a geometrically simple and structurally well-defined experimental model is particularly strong because, at present, accurate and quantitative theories exist only for simple geometries such as cylindrical or slit pores.[13,14] Moreover, single-pore membranes allow measurement of the temporal response of a single pore, which is useful for obtaining stochastic information about transport parameters or for investigating time-dependent properties such as voltage- or chemically induced gating.[5,15] Single nanopores consisting of membrane proteins have been extensively studied previously.[16] However, these protein channels are dynamically complex structures and may not be good models for testing existing theories. At present, even transport for simple ions is not well-understood because of the complexity, fluidity, and instability of protein structures.

Two challenges are often encountered when relying on single-pore membrane models for transport studies. First, very few methods exist that allow convenient fabrication of single-pore membranes with pore dimensions on the nanometer scale. Second, only an extremely small amount of materials can be transported through a single nanopore, which implies that a very sensitive analytical method is needed for measuring the transport rate. Here, we present our latest efforts in meeting the above challenges: the development of a simple template method for fabricating membranes containing a single pore of about 150 nm inside diameter, and the application of Coulter counting principle to transport measurements.

Experimental Section

Fabrication of Single-Nanopore Membranes. The carbon nanotube used here consists of a crystalline multiwalled graphitic tube coated with an amorphous carbon layer.[17] Single carbon nanotubes were mounted on a macroscopic metal wire using an established method.[18,19] The nanotube was then embedded in epoxy matrix (Epo-Fix, EMS, Fort Washington, PA), microtomed (UltraCut E, Reichert-Jung), and imaged (Zeiss 10C or JEOL JEM-2010). A typical nanopore-containing section was mounted, with the aid of an optical microscope (Optiphot, Nikon) and a translational stage (model 462: Newport, Irvine, CA), onto a single-hole (about 5 μm diameter) $Si(100)/Si_3N_4$ support structure (12.5 mm by 12.5 mm square piece with a thickness of 525 μm) that was micro-machined using standard MEMS technologies.[20]

Measurements of Probe-Particle Transport. All aqueous solutions were prepared with analytical grade reagents and water of 18.2 MΩ-cm resistivity (Milli-Q, Millipore), and filtered through a 0.2 μm syringe filter (Acrodisc, Gelman Sciences). Triton-X 100 (Sigma Chemical) was used to facilitate filling of the nanotube with aqueous solutions and to stabilize the polystyrene probe spheres (±10 nm uncertainty in diameter, Bangs Laboratories, Fishers, IN). A membrane sample was clamped between two half cells with a silicone O-ring seal. The cells were made of polycarbonate (LEXAN), and the volume of each cell chamber was about 0.3 mL. The current was measured in voltage-clamp mode with an integrated data acquisition system (Axopatch 200B and Digipack 1200, Axon Instruments, Foster City, CA). In a typical experiment, the cell chambers were filled with electrolytes with no probe spheres. A linear cyclic voltammogram was then obtained to verify that the pore is conducting and that its length, as calculated based on ionic conductivity (see below), falls within the expected range which was controlled with thickness settings on the microtomer. After this, the electrolyte in one cell chamber was replaced with the same electrolyte except that it contains probe spheres at a concentration of 5.0×10^{11} spheres/mL. Coulter counting experiments were followed immediately with the entire cell-assembly enclosed in a faraday cage (model 81-323-03, TMC, Beabody, MA).

Data Analysis. Current versus time traces were processed with a custom-written software program and with Microsoft Excel. Pulse selection and noise rejection were gauged with a set of user-specified criteria such as minimum pulse width and minimum pulse height. In addition to the inherent uncertainty characteristic of events that follow Poisson statistics (see below), the number of pulses counted by the software could vary slightly due to the subjective nature of the pulse-selection criteria. The relative error in flux measurements due to software is typically 5% for a high-S/N ratio trace and 20% for the most noisy trace.

Results and Discussions

Figure 1 illustrates the template method for fabricating membranes that contain only a single nanopore. This method has several attractive features. First, the geometric and chemical properties of the nanopore are well-defined because of the unique characteristics of carbon nanotubes. For example, the pore diameter is uniform along the entire pore length, and a set of nanoporous membranes of essentially identical diameter can be obtained if they are all derived from a common nanotube. This is a clear advantage over most lithographic methods in which very tight control over fabrication conditions is required to achieve identical replicates. Additionally, the inner wall of a nanopore is an atomically smooth graphitic sheet, which is perhaps the best approximation of some simple theoretical models that assume a "structureless" wall. Second, the single nanotube is embedded within a highly stable polymeric matrix, which is a good insulator for both electron and ion conduction. This means that interference due to leakage and Faradaic currents will be minimized when the nanopore is configured as a Coulter counter for rate measurements.[6] Finally, many nanopore membranes can be prepared rapidly due to the efficiency of the dicing approach (Figure 1B). This greatly enhances reproducibility and reduces sample preparation time, making the method practical for routine studies.

(12) Schönenberger, C.; van der Zande, B. M. I.; Fokkink, L. G. J.; Henny, M.; Schmid, C.; Krüger, M.; Bachtold, A.; Huber, R.; Birk, H.; Staufer, U. *J. Phys. Chem.* **1997**, *101*, 5497−5505.
(13) Deen, W. M. *AICheE J.* **1987**, *33*, 1409−1425.
(14) Xu, L.; Sedigh, M. G.; Sahimi, M.; Tsotsis, T. T. *Phys. Rev. Lett.* **1998**, *80*, 3511−3514.
(15) Fyles, T. M.; Loock, D.; Zhou, X. *J. Am. Chem. Soc.* **1998**, *120*, 2997−3003.
(16) See, for example: Taglialatela, M.; Wible, B. A.; Caporaso, R.; Brown, A. M. *Science* **1994**, *264*, 844−847.
(17) Alig, R. L.; Burton, D. J. Carbon '97, 23rd Biennial Conference on Carbon, July, 1997.
(18) Campbell, J. K.; Sun, L.; Crooks, R. M. *J. Am. Chem. Soc.* **1999**, *121*, 3779−3780.
(19) Wong, S. S.; Woolley, A. T.; Joselevich, E.; Cheung, C. L.; Lieber, C. M. *J. Am. Chem. Soc.* **1998**, *120*, 8557−8558.
(20) *Semiconductor Sensors*; Sze, S. M., Ed.; Wiley: New York, 1994.

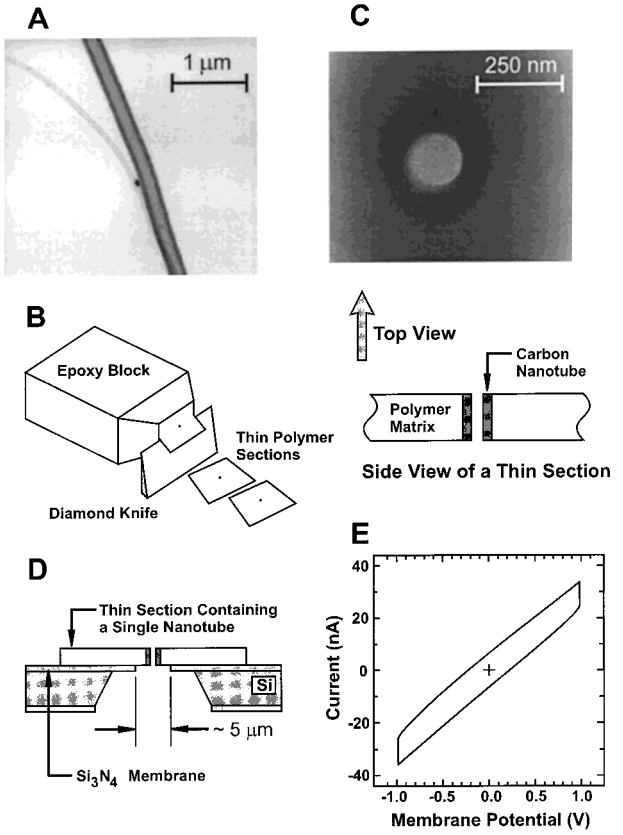

Figure 1. Fabrication and characterization of single-pore membranes. A multiwall carbon nanotube, as seen in the TEM image (A), has a very uniform pore diameter over a length greater than 100 μm. After being embedded in an epoxy block, the nanotube is microtomed perpendicular to its long axis (B) and a representative section is then imaged by TEM to determine accurately the pore diameter (C). A single-pore membrane is prepared by fixing a nanotube-containing section onto a Si_3N_4 support (D). The pore length can be calculated from eq 1 using the TEM pore diameter and the conductance determined using cyclic voltammetry (E). For this particular sample, the inside diameter of the nanopore is 153 nm, and the pore length is 660 nm.

Measuring mass transport rates through a single nanopore is normally very difficult. However, a simple but sensitive method is available, which is based on the Coulter counting principle.[21] A Coulter counter detects a probe by monitoring the current pulse induced by the probe as it moves across the single pore.[22] In the absence of the probe, the baseline ionic current, i_P, is

$$i_P = \frac{\kappa\pi d_P^2 \Delta E_P}{4(l_P + 0.9d_P)} \quad (1)$$

where ΔE_p is the voltage across the membrane, κ is the electrolyte conductivity, d_P is the pore diameter, and l_P is the pore length. The current pulse, Δi_P, induced by the probe is

$$\frac{\Delta i_P}{i_P} = S(d_P, d_S)\frac{d_S^3}{(l_P + 0.8\,d_P)d_P^2} \quad (2)$$

where d_S is the diameter of the probe sphere, and $S(d_P, d_S)$ is a correction factor that depends on d_P and d_S.

Coulter counting can provide a wide variety of information about mass-transport kinetics. Figure 2 shows typical current-versus-time traces obtained in a Coulter counting experiment. For example, each current pulse (downward spike) in the upper trace of Figure 2B corresponds to a single transport event as the polystyrene probe is driven through the carbon nanotube under a constant electric field gradient. The current pulses do not arise from noise because (a) they are easily distinguished from the random baseline noise, (b) consistent with the Coulter counting principle, all pulses point in the same direction, which corresponds to a decrease in the absolute membrane current, and (c) no pulse was detected when charged probes were prevented from entering the nanopore by switching the direction of the electric field (the lower trace of Figure 2B).

The size of every probe particle transported through the pore can be calculated using eq 2, and the velocity of the probe can be calculated from the pulse width. Unfortunately, with the present experimental setup, these parameters cannot be reliably obtained because the average transit time of a probe within the nanotube is shorter than the instrument time resolution (we do not fully understand why the time resolution is limited to about 1 ms). Thus, the observed pulse height is smaller than the value predicted using eq 2. However, better agreement was found when the average transit time was increased by slowing down the probe using a pressure gradient opposite to the direction of probe transport (see Supporting Information, Figure S1).

In addition to direct calculation from measured pulse widths, the average probe velocity, v_S, can also be found from the probe flux, J_S:

$$v_S = \frac{4J_S}{\pi c_S d_P^2} \quad (3)$$

where c_S is the probe sphere concentration. The observed velocity, v_S, may be broken down into four terms, which correspond to contributions from hydrodynamic transport,[23] electrophoretic and electroosmotic transport,[24] and diffusion:[25,26]

$$v_S = \frac{d_P^2}{32\eta l_P}\Delta P + \frac{\mu_S}{l_P}\Delta E_M - \frac{\epsilon\zeta_P}{4\pi\eta l_P}\Delta E_M + \frac{D_S}{c_S l_P}\Delta c_S \quad (4)$$

where η and ϵ are medium's viscosity and dielectric constants, respectively; μ_S and D_S are probe sphere's electrophoretic mobility and diffusion coefficient, respectively; and ζ_P is the zeta potential of the pore surface.

The first and the third terms of eq 4 are not completely independent of one another: for example, a hydrodynamic flow across a charged pore will induce a streaming potential.[24] Our streaming potential measurements indicate that the inner surface of the carbon nanopore is essentially neutral (-1 mV $< \zeta_P <$ 0 mV); thus, the electroosmotic transport plays a less dominant role compared to the hydrodynamic and electrophoretic components. In this study, diffusion is the slowest transport mode (about 10 μm/s based on eq 4 and an estimated Stokes−Einstein diffusion coefficient).

(21) Lines, R. W. In *Particle Size Analysis*; Stanley-Wood, N. G., Linew, R. W., Eds.; Royal Society of Chemistry: Cambridge, 1992; pp 351−383.
(22) DeBlois, R. W.; Bean, C. P. *J. Colloid Interface Sci.* **1977**, *61*, 323−335.
(23) Fetter, A. L.; Walecka, J. D. *Theoretical Mechanics of Particles and Continua*; McGraw-Hill: New York, 1980.
(24) Probstein, R. F. *Physicochemical Hydrodynamics*: *An Introduction*; Butterworth: Boston, 1989.
(25) Bard, A. J.; Faulkner, L. R. *Electrochemical Methods, Fundamentals and Applications*; Wiley: New York, 1980.
(26) The diffusional velocity is obtained from diffusional flux by assuming a constant concentration gradient of $\Delta c_S/l_P$.

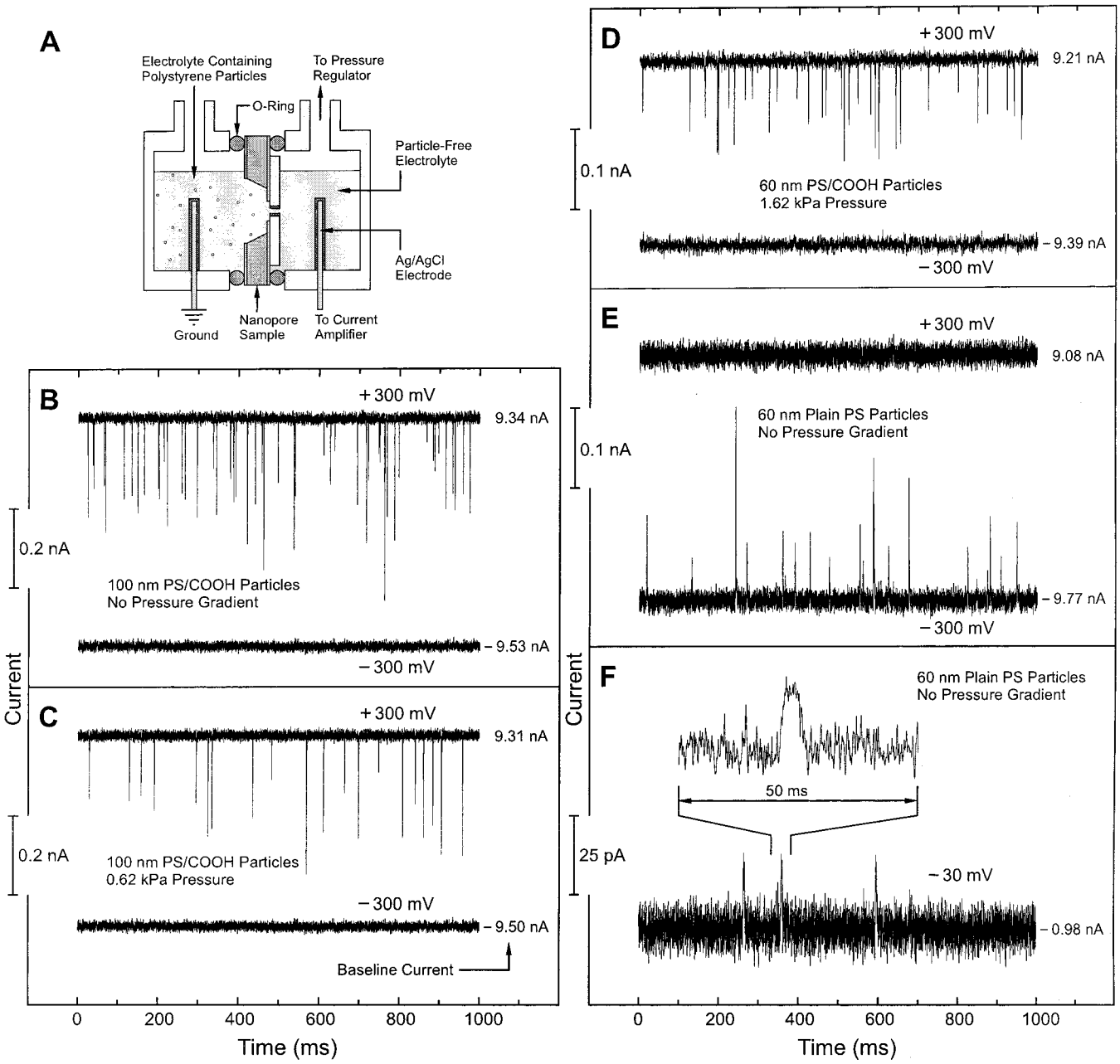

Figure 2. Measurements of mass transport rate using the Coulter counting method and the membrane used to obtain the data shown in Figure 1E. The measurement cell consists of two chambers separated by a nanopore membrane: each chamber encloses a freshly prepared Ag/AgCl electrode and an electrolyte containing 0.1 M KCl, 0.1% (w/v) Triton X-100, and 10 mM pH 7 phosphate buffer (A). The right chamber is connected to a water-filled barometer for pressure control and readout, and the left chamber is loaded with polystyrene probe particles. Negatively charged probe particles, such as 100 nm-diameter, COOH-modified particles (B), are transported through the nanopore only when a +300 mV voltage is applied (B, top trace). No particle is detected when a −300 mV voltage is applied, as one would expect for electrophoretic transport (B, bottom trace). The particle flux, or the average particle velocity, can be reduced when a pressure gradient opposing the electrical field gradient is applied (C). Smaller probe spheres (60 nm diameter, COOH-modified) can also be detected although they move faster and the average pulse height is smaller (D). Nominally neutral probe spheres (60 nm diameter with no charged surface groups) are actually positively charged in our experiments (see text) (E). However, they carry smaller surface charge and move more slowly than COOH-modified spheres of the same diameter. At low driving voltages, the velocity of these particles is further attenuated, making it possible to reliably measure the pulse width, a more direct measure of transport rate than the flux (F).

The contributions from hydrodynamic and electrophoretic transport can be evaluated separately. For example, the rate constant, K_P, (coefficient of the first term in eq 4) for the hydrodynamic transport can be measured by maintaining a constant rate of electrophoretic transport (Figure 3A). The measured K_P (1.7×10^{-4} cm s^{-1} Pa^{-1}) agrees approximately with the calculated value (1.1×10^{-4} cm s^{-1} Pa^{-1} from eq 4). However, further study is required to explain the large relative discrepancy between these two values. Similarly, the electrophoretic rate constant, K_E (coefficient of the second term in eq 4) can be calculated independently from the slope of a flux-versus-membrane potential plot (Figure 3B). An unexpected finding is that neutral polystyrene probes carry an effective positive surface charge (Figure 2 D and E). We hypothesize that the positive charge originates from K^+ ions, which are concentrated near particle surfaces through crown-ether-like interactions with particle-bound Triton X-100 surfactant. The electrophoretic mobility of these positively charged probes is

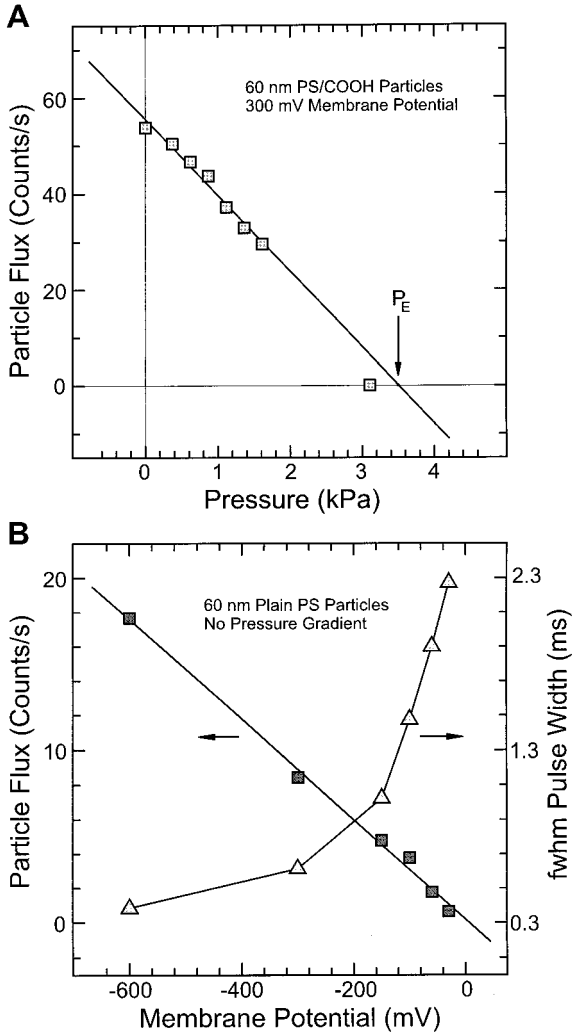

Figure 3. Measurements of hydrodynamic and electrophoretic transport rates. (A) The hydrodynamic transport rate (eq 4) can be calculated using eq 3 and the slope of the flux vs. pressure plot (squares are experimental data and the line is the best fit) at a constant electric field gradient. P_E corresponds to the pressure at which hydrodynamic and electrophoretic flow are exactly canceled out. (B) Similarly, the electrophoretic transport rate can be obtained from the flux vs. voltage plot. The pulse width (fwhm = full width at half-maximum) cannot be resolved at high particle velocity (or high driving voltage) because of instrumental and noise limitations. However, at low velocity, the pulse width can be measured reliably and is inversely proportional to the particle velocity (eq 4).

2.1×10^{-5} cm^2 s^{-1} V^{-1}, which is calculated according to eq 4 using the values of measured pore length (660 nm) and electrophoretic rate constant (3.15×10^{-1} cm s^{-1} V^{-1} from Figure 3B).

The single-pore transport data presented here can be analyzed statistically (Figure 4). Such analysis allows us to answer the question of whether a probe particle will enter a pore several times before leaving it completely. This question cannot be answered by analyzing each individual pulse in a Coulter counting experiment, but it can be answered by statistical analysis. Chiu and Zare observed that fluorescent polystyrene spheres enter the focal point of an exciting laser beam more frequently than what would be expected if the arrival of the spheres is completely random.[27] This so-called biased diffusion is caused by the optical trapping effect, which tends to favor the reentry of a sphere at short times after its first visit to the laser detection zone. The nanopore in a Coulter counter can be thought as an electrochemical detecting zone. The arrival of probe spheres to this zone is expected to be completely random, even though in our case the spheres are driven to this zone mainly by an electrical field instead of by diffusion. If there exists a trap field (just like the optical trapping field) that favors reentry of a probe spheres after its first entry into the nanopore, then pulse counting would deviate from Poisson statistics. No such deviation was found within a time period comparable to the longest waiting time between two neighboring pulses (Figure 4). Thus, most particles only enter the pore once, under the conditions used in this work.

(27) Chiu, D. T.; Zare, R. N. *J. Am. Chem. Soc.* **1996**, *118*, 6512−6513.

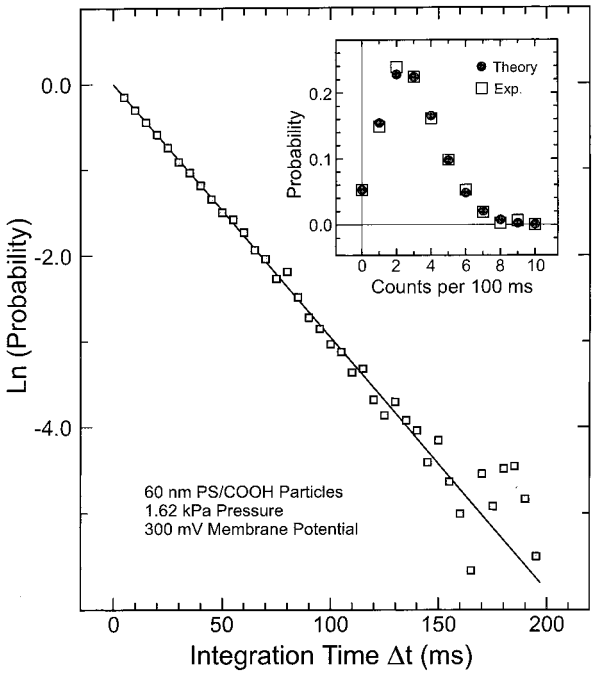

Figure 4. The transport of probe particles follows Poisson statistics: $p(k, \lambda\Delta t) = e^{-\lambda\Delta t}(\lambda\Delta t)^k/k!$, where λ is the average number of pulses (or counts) per second, and $p(k, \lambda\Delta t)$ is the probability of observing k counts in an integration time window of Δt. A long train of pulses, such as those shown in Figure 2, are recorded and $p(k, \lambda\Delta t)$ are measured as $N(k)/N(\text{total})$, where $N(k)$ is the number of Δt windows that contain k counts and $N(\text{total})$ is the total number of Δt windows processed. $p(k, \lambda\Delta t)$ can also be calculated theoretically according to the above equation using only the average counts per window ($\lambda\Delta t$) as the input parameter. The experimentally measured and calculated $p(k, \lambda\Delta t)$ agree with one another in both the $\ln[p(0, \lambda\Delta t)]$ vs. Δt plot (the large graph) and the $p(k, \lambda\Delta t)$ vs. k plot (the inset with $\Delta t = 100$ ms).

Conclusions

The results reported here clearly demonstrate that quantitative information about mass transport can be obtained from single-nanopore models. This will open up many avenues for further investigation of the correlation between the transport rate and the structures of the probe and the pore. For example, it will be interesting to modify the inner surface of a carbon nanopore with an anionic surfactant, such as sodium dodecyl sulfate, thereby rendering it negatively charged. This is expected to enhance electroosmotic transport.

We believe that the pore diameter can be reduced by up to a factor of 10 using the fabrication method presented here. This will have two significant consequences. First, it will bring measurements closer to the critical dimension below which mass transport will deviate from conventional continuum models. For example, the specific molecular structure of the inner nanopore

surface will become more important in determining the transport rate and in causing deviation of continuum properties, such as viscosity, from their bulk values.[28,29] Second, reduction in pore diameter will permit construction of molecular Coulter counters.[6,30,31] For example, a 15 nm-diameter pore should allow us to detect large polymeric molecules such as dendrimers, antibodies, and viruses. Molecular Coulter counters will create many new opportunities for chemical analysis because many molecules such as proteins, polysaccharides, and DNA do not have the desirable electrochemical or spectroscopic properties that are often required by present-day analytical detectors.

(28) Magda, J. J.; Tirrell, M.; Davis, H. T. *J. Chem. Phys.* **1985**, *83*, 1888−1901.
(29) Ballard, L.; Jonas, J. *Langmuir* **1996**, *12*, 2798−2801.
(30) Kasianowicz, J. J.; Brandin, E.; Branton, D.; Deamer, D. *Proc. Natl. Acad. Sci. U.S.A.* **1996**, *93*, 13770−13773.
(31) Gu, L.-Q.; Braha, O.; Conlan, S.; Cheley, S.; Bayley, H. *Nature* **1999**, *398*, 686−690.

Acknowledgment. We gratefully acknowledge financial support from the National Science Foundation (CHE-9796203 and CHE-9818302). We thank Dr. D. G. Glasgow (Applied Sciences, Inc., Cedarville, OH) for providing the carbon nanotubes, Kevin Roberts (University of Minnesota) for assistance in clean-room device fabrication, and Helga Sittertz-Bhatkar (Texas A&M University) for assistance in microtoming and TEM imaging.

Supporting Information Available: Histograms of probe diameters calculated using measured pulse heights and eq 2 (PDF). This material is available free of charge via the Internet at http://pubs.acs.org.

JA002429W